

Cite this article as: Yang Mei, Liu Liangwen, Zheng Heng, et al. Loading Mechanism and Loading Kinetics of TiO₂ on Cordierite Surface by Chemical Vapor Deposition[J]. Rare Metal Materials and Engineering, 2022, 51(03): 778-782.

ARTICLE

Loading Mechanism and Loading Kinetics of TiO₂ on Cordierite Surface by Chemical Vapor Deposition

Yang Mei¹, Liu Liangwen¹, Zheng Heng², Lu Jingxiang¹, Wang Jingyi¹

¹ School of New Energy and Materials, Southwest Petroleum University, Chengdu 610500, China; ² State Key Laboratory of Industrial Vent Gas Reuse, Southwest Research & Design Institute of Chemical Industry, Chengdu 610225, China

Abstract: In order to explore the loading mechanism and loading kinetics of TiO₂ on cordierite, the acid-etched cordierite was used as the matrix and the TiO₂ loading test was conducted by the chemical vapor deposition (CVD) method. The scanning electron microscope, energy disperse spectroscopy, X-ray diffraction, and Brunauer-Emmett-Teller (BET) specific surface area measurement were used to characterize the TiO₂ on cordierite surface and determine the loading speed at different temperatures. The results show that the surface of modified cordierite with TiO₂ mainly consists of (211)-oriented and (200)-oriented anatase-TiO₂ which is the octahedron and cube with BET specific surface area of 78.80 m²·g⁻¹, an average pore diameter of 9.80 nm, and a bimodal distribution. The loading process is the diffusion and adsorption of TiCl₄ and O₂ towards the cordierite matrix. TiCl₄ decomposes and Ti⁴⁺ enters the matrix lattice under the high oxygen potential to form TiO₂ nuclei. After the preferential orientation and epitaxial growth, the loading deposition rate equation is $V = 6807 \exp\left(-\frac{7255}{T}\right) P_{\text{TiCl}_4}^0$, where T is the loading temperature and $P_{\text{TiCl}_4}^0$ is the partial pressure when TiCl₄ is in the gas phase.

Key words: catalyst; SCR; CVD; TiO₂; loading kinetics

A large amount of NO_x in the exhaust gas of coal-fired power plants has a serious damage to the environment and human health^[1,2]. Currently, the selective catalytic reduction (SCR) with a wide reaction temperature range, high denitration efficiency, good selectivity, and good operational safety is an effective way to control NO_x pollution, and it is also a commonly used flue gas denitration method with the technical core of catalysts^[3]. The metal oxide catalysts have been widely investigated in recent years, and the vanadium oxide attracts much attention^[4-9].

The commonly used commercial catalysts are monolithic V₂O₅-WO₃/TiO₂, and the content of TiO₂-carrier accounts for more than 80%^[10]. V₂O₅ is the main active component of SCR denitration reaction, which needs to be loaded on a suitable carrier surface; otherwise, the SCR denitration efficiency will be negatively influenced. The activity and selectivity of V₂O₅ are also sensitive to the carrier. Only a few oxides, such as TiO₂, Al₂O₃, and SiO₂, have good surface dispersion. Most

researches focus on the addition of different elements into the V₂O₅-WO₃/TiO₂, such as the alkali metals, alkaline earth metals, and other elements (As, Pb, Zn, S, P)^[11-18]. TiO₂ is usually loaded on the surface of a low-cost porous matrix to reduce the total content of TiO₂ in the carrier^[19-21], and the loading method is sol-gel method. However, this method has low loading efficiency of TiO₂, uneven dispersion, and poor bonding to the matrix. The TiO₂ film or TiO₂ particle treated by chemical vapor deposition (CVD) for photocatalysts has the advantages of high bonding strength, uniform dispersion, and large Brunauer-Emmett-Teller (BET) specific surface area^[22]. Woods et al^[23] applied CVD method on Ti(NMe₂)₄ and O₂ as the precursors at 250~300 °C, and the TiO₂ film was obtained after annealing at 600 °C. Wang et al^[24] reported that TiN and TiO₂ are directly deposited on the surface of 310S stainless steel with the dimension of 10 mm×10 mm×0.9 mm by atmospheric pressure CVD method. Kuo et al^[25] reported that the crystalline titanium oxide films with a thickness of

Received date: March 21, 2021

Foundation item: Sponsored by State Key Laboratory of Industrial Vent Gas Reuse (SKLIVGR-SWPU-2020-04)

Corresponding author: Yang Mei, Ph. D., Professor, School of New Energy and Materials, Southwest Petroleum University, Chengdu 610500, P. R. China, E-mail: 199631010016@swpu.edu.cn

Copyright © 2022, Northwest Institute for Nonferrous Metal Research. Published by Science Press. All rights reserved.

0.09~0.55 μm are prepared below 500 $^{\circ}\text{C}$ by CVD method with a mixture of titanium tetrachloride (TiCl_4), carbon dioxide (CO_2), and hydrogen (H_2).

Although the preparation of TiO_2 by CVD has been widely studied, the loading mechanism and loading kinetics of TiO_2 by CVD on cordierite matrix are still unclear. This research investigated the loading mechanism and loading kinetics of TiO_2 on the surface of honeycomb ceramics of modified cordierite, and provided theoretical basis for further CVD application.

1 Experiment

The honeycomb cordierite ceramic was used, and its main chemical composition is MgO (17.2wt%), Al_2O_3 (30.2wt%), and SiO_2 (51.1wt%). The cordierite was acid-treated (HNO_3) at 110 $^{\circ}\text{C}$ for 6 h. Then the modified cordierite was cut into small specimens of 20 mm \times 20 mm \times 30 mm as the matrix material for CVD. The physical properties of the modified cordierite are shown in Table 1.

The titanium tetrachloride (TiCl_4) and O_2 were used as the reaction precursors for CVD treatment. TiCl_4 was vaporized at 35 $^{\circ}\text{C}$ with a carrier gas of N_2 . Then N_2 for dilution was added to control the gas flow and flow rate. The flow of N_2 carrier gas, N_2 for dilution, and O_2 was 500, 1000, and 80 mL/min, respectively. The pressure was maintained at the standard atmospheric pressure, the reaction time was 10 min, and the loading temperature (T) was 450 $^{\circ}\text{C}$.

The BET specific surface area and pore structure of the catalyst were measured by the 1990-type N_2 physical adsorption instrument. TESCAN VEGA2 variable vacuum scanning electron microscope (SEM) was used to observe the morphology of specimens. INCA Energy 350 X-ray energy disperse spectrometer (EDS) was used to analyze the composition. The Rigaku D/max-3C X-ray diffractometer (XRD) was used for structure and phase analysis. The loading speed was calculated through the specimen mass before and after loading by an electronic balance. The metallographic

microscope (DME-300M) was also used for microstructure observation. The bonding strength between the TiO_2 layer and the acid-modified cordierite was tested on the specimens of 20 mm \times 10 mm \times 5 mm, and the bonding force was measured by MFT-4000 surface scratch.

2 Results and Discussion

2.1 Characterization of TiO_2 -loaded cordierite

The properties of TiO_2 -loaded cordierite are shown in Table 1. All TiO_2 -loaded cordierite specimens have a porous surface with BET specific surface area of 78.80 $\text{m}^2\cdot\text{g}^{-1}$, and the total porous area is 72.76 $\text{m}^2\cdot\text{g}^{-1}$. The total pore volume is 0.2018 $\text{cm}^3\cdot\text{g}^{-1}$. The pore size distribution of TiO_2 -loaded cordierite is shown in Fig.1. Most TiO_2 -loaded cordierite has the pore size of 3~25 nm, and the peak pore size is 9~11 nm. The average pore size is 9.80 nm, and the pore size distribution has the bimodal characteristic, which provides a good structure condition for the loading of active components.

SEM morphologies of the cordierite matrix with and without TiO_2 are shown in Fig.2. The surface microstructure changes due to the macroscopic properties of the modified cordierite matrix.

Before loading TiO_2 , the surface of the modified cordierite matrix has many macropores and a few micropores. After loading TiO_2 , the surface of the modified cordierite matrix still has many large pores, whereas the number of micropores is greatly increased. The entire surface is evenly covered by TiO_2 , and many ravines are filled. The large increase in micropores causes the increase in BET specific surface area, and the change in linear expansion coefficient is also closely related to the uniform coverage of TiO_2 . The surface of cordierite matrix consists of agglomerated particles, thereby forming a clump-like structure. The diameter of the clumps varies from 1 μm to 2 μm . There are many small micropores between the particles. Some large pores with the diameter of 4~6 μm are formed, which is in good agreement with the pore size distribution in Fig.1.

Table 1 Properties of modified cordierites with and without TiO_2

Specimen	BET specific surface area/ $\text{m}^2\cdot\text{g}^{-1}$	Total porous area/ $\text{m}^2\cdot\text{g}^{-1}$	Total pore volume/ $\text{cm}^3\cdot\text{g}^{-1}$	Average pore diameter/nm
Modified cordierite	46.18	37.32	0.0447	4.82
Modified cordierite with TiO_2	78.80	72.76	0.2018	9.80

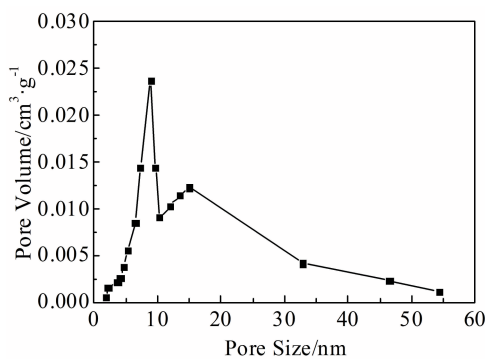


Fig.1 Pore size distribution of TiO_2 -loaded cordierite

The phase components of TiO_2 -loaded cordierite at 450 $^{\circ}\text{C}$ were analyzed by XRD and EDS. XRD pattern is shown in Fig.3. The main phases are the cordierite matrix ($\text{Mg}_2\text{Al}_4\text{Si}_5\text{O}_{18}$) and anatase- TiO_2 . The peaks of anatase- TiO_2 are at $2\theta = 25.381^{\circ}$, 37.80° , 48.049° , 62.688° , and no obvious crystal plane of (011) orientation can be observed. The main elements are O and Ti, suggesting that anatase- TiO_2 is successfully loaded on the cordierite matrix by CVD method. Anatase- TiO_2 is a tetragonal crystal, and its unit cell model mainly has three crystal plane orientations: (211), (200), and (211). The unit cell appears as an octahedron when all crystal planes are (211)-oriented, and the final crystal grains also appear as an

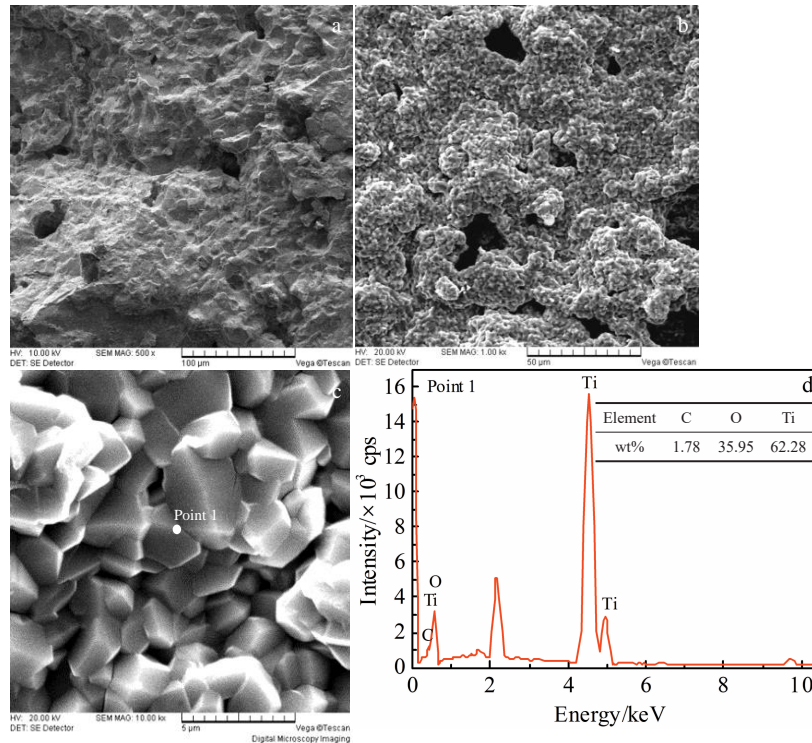


Fig.2 SEM morphologies (a, b) and EDS analysis (c) of modified cordierites without (a) and with (b, c) TiO_2 ; EDS results of point 1 in Fig.2c (d)

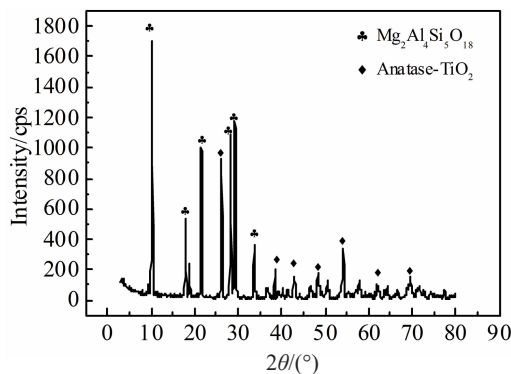


Fig.3 XRD pattern of TiO_2 -loaded cordierite

octahedron. When the crystal planes are all (200)-oriented, the unit cell appears as a cube with the final cubic crystal grains. It can be inferred from the octahedral and cubic morphologies of anatase- TiO_2 that the loaded TiO_2 has the crystal orientations of mainly (211) and (200). After the formation of TiO_2 crystal nuclei on the surface of cordierite matrix during CVD process, the growth of TiO_2 crystal grains suffer the orientation elimination and adjustment, forming the preferred (211) and (200) orientations. The final grain growth method is epitaxial growth, and the TiO_2 crystal covers the surface of cordierite matrix.

A trace amount of C can be observed in Fig.2d, because the matrix contains impurities, which diffuse to the surface during CVD process. The bonding strength results are shown in Fig.4. The bonding strength between TiO_2 and the modified cordierite matrix reaches 28 N.

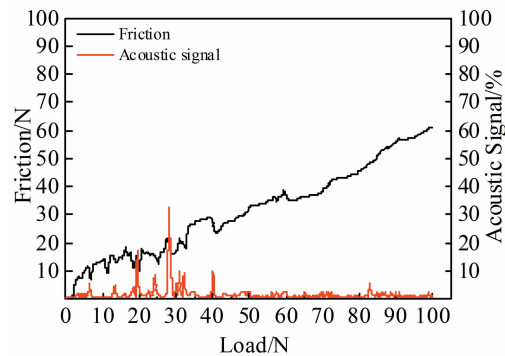
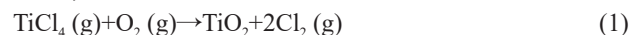


Fig.4 Bonding force of TiO_2 -loaded cordierite

2.2 Thermodynamic calculation of CVD method

The reaction system was TiCl_4 , O_2 , and carrier gas N_2 in this research, and the reaction is as follows:



According to the thermodynamic formula, the free energy of reaction is as follows:

$$\Delta_r H_m^\theta(298 \text{ K}) = -180 \text{ kJ/mol} \quad (2)$$

$$\Delta_r G_m^\theta(298 \text{ K}) = -162.5 \text{ kJ/mol} \quad (3)$$

where $\Delta_r H_m^\theta(298 \text{ K})$ is the standard molar enthalpy change of Eq.(1) at 298 K; $\Delta_r G_m^\theta(298 \text{ K})$ is the molar Gibbs free energy of Eq.(1) at 298 K. It can be seen from the calculation results at room temperature (298 K), the thermodynamics does not restrict the reaction, but the kinetic factor is the main factor controlling the entire reaction process.

2.3 Analysis of loading mechanism and loading kinetics

The mixture gas of TiCl_4 and O_2 accompanied by carrier gas is diffused into the cordierite matrix during the first stage of

CVD process. Excess O₂ mainly plays a role in maintaining the oxygen potential. TiCl₄ decomposes on the cordierite matrix: TiCl₄→Ti⁴⁺+4Cl⁻. Then Cl⁻ agglomerates to form Cl₂, thereby leaving cordierite matrix and the reaction system.

The ionic radius of Mg²⁺, Al³⁺, Si⁴⁺, and Ti⁴⁺ in the cordierite matrix is 0.089, 0.053, 0.040, and 0.065 nm, respectively. Because the ion size of Ti⁴⁺ is closer to that of Al³⁺ and Si⁴⁺, the displacement reaction can easily cause Ti to enter the cordierite lattice. After the acid etching modification of cordierite, the alkaline Mg²⁺ and the neutral Al³⁺ are lost on the surface of the cordierite matrix, and the acidic Si⁴⁺ ions are abundant. Si⁴⁺ is mainly distributed in the pore parts of the cordierite matrix with a smaller radius of curvature, indicating that its surface energy is high and it is in an unbalanced state. Due to the existence of a large amount of high-energy silicon dioxide, Ti⁴⁺ ions firstly replace Si⁴⁺, and the lattice oxygen forms a covalent bond with the titanium and oxygen. Excess oxygen in the atmosphere maintains the high oxygen potential to keep Ti⁴⁺ and form the anatase-TiO₂ crystal structure.

During the formation of Ti-O on the cordierite surface, the diffusion of the interface layer in cordierite surface and the deposition of Ti diffusion are involved. The diffusion capacity is affected by temperature and can influence the reaction rate. In addition, the reaction process is affected by the temperature and the partial pressure of the components in the system. Thus, CVD process is controlled by kinetics.

2.4 Establishment of kinetic model

To establish the loading kinetic model, the deposition rate *V* (g·cm⁻²·h⁻¹) obtained by the loading tests at different loading temperatures *T* (523.15, 573.15, 623.15, 673.15, 723.15, 773.15, and 823.15 K) is used, as listed in Table 2.

It can be seen that the deposition rate is increased with increasing the loading temperature, based on the preliminary judgement of a dynamic control process. The relationship between deposition rate and loading temperature is shown in Fig.5, and the fitting equation is as follows:

$$\ln V = 8.82571 - 7255.721/T \tag{4}$$

According to Arrhenius formula:

$$K = A_0 \exp\left(-\frac{\Delta E_a}{RT}\right) \rightarrow \ln(K) = \ln(A_0) - \frac{\Delta E_a}{RT} \tag{5}$$

where *A*₀ is the frequency factor; *K* is the rate constant of activation process; *E*_a is the activation energy; *R* is the molar gas constant.

Table 2 TiO₂ loading speeds at different loading temperatures

Loading temperature/K	Mass gain of cordierite matrix/g	Deposition rate, <i>V</i> /g·cm ⁻² ·h ⁻¹
523.15	0.024	0.008
573.15	0.051	0.017
623.15	0.120	0.040
673.15	0.600	0.200
723.15	1.110	0.370
773.15	1.680	0.560
823.15	2.670	0.890

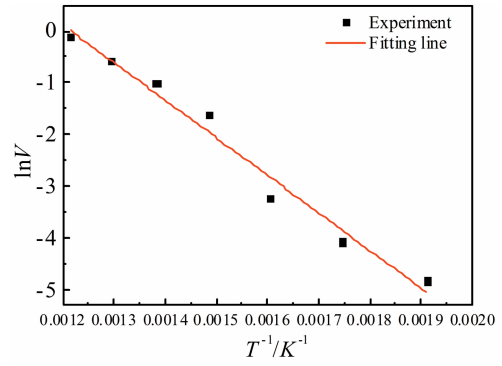


Fig.5 Kinetics of deposition rate and loading temperature

Based on the fitting equation, the average activation energy at 250~550 °C is 60.3 kJ/mol, and the frequency factor *A*₀=6807/s. From the previous analysis, CVD is mainly composed of three key steps (the influence of other processes on deposition is not considered).

Step 1: TiCl₄ and O₂ are adsorbed, diffused, and migrate on the cordierite matrix. Because O₂ is excessive and maintains the sufficient partial pressure, only the partial pressure of TiCl₄ and the reaction rate are considered:

$$V_{TiCl_4} = H_{TiCl_4} (P_{TiCl_4}^0 - P_{TiCl_4}) \tag{6}$$

where *V*_{TiCl₄} is reaction rate of TiCl₄; *H*_{TiCl₄} is mass transfer coefficient of TiCl₄; *P*_{TiCl₄}⁰ is the partial pressure when TiCl₄ is in the gas phase; *P*_{TiCl₄} is the partial pressure of TiCl₄ on the surface of cordierite substrate.

Step 2: based on Eq.(6), the reaction rate of TiO₂ deposition and Cl₂ generation can be obtained, as follows:

$$V_{TiO_2} = k_f P_{TiCl_4} - k_c P_{Cl_2} \tag{7}$$

where *V*_{TiO₂} is the net reaction rate of TiO₂ generation; *k*_f is the positive response coefficient; *k*_c is the inverse reaction coefficient; *P*_{Cl₂} is the partial pressure of Cl₂ at the surface of the cordierite substrate.

Step 3: Cl₂ (the initial partial pressure is 0 Pa) is diffused from the deposition zone of the cordierite surface:

$$V_{Cl_2} = h_{Cl_2} (P_{Cl_2} - P_{Cl_2}^0) \tag{8}$$

where *V*_{Cl₂} is diffusion rate of the product Cl₂ away from the substrate; *h*_{Cl₂} is the mass transfer coefficient of Cl₂; *P*_{Cl₂} is the partial pressure when Cl₂ is in the gas phase.

When the chemical vapor deposition of TiO₂ is in a stable stage, the system is balanced and the deposition rates of different components are equal:

$$V_{TiCl_4} = V_{TiO_2} = V_{Cl_2} = V \tag{9}$$

The deposition rate *V* is measured value from the tests. Because both TiCl₄ and Cl₂ are diffused through the entire reaction system, their diffusion coefficients are equal. Therefore, Eq.(10~12) can be obtained, as follows:

$$V = k_f P_{TiCl_4}^0 \tag{10}$$

$$k_f = A \exp\left(-\frac{\Delta E_0}{RT}\right) \tag{11}$$

$$V = \exp\left(-\frac{\Delta E_0}{RT}\right) P_{TiCl_4}^0 = 6807 \exp\left(-\frac{7255}{T}\right) P_{TiCl_4}^0 \tag{12}$$

where A is the frequency factor; T is the loading temperature and $P_{\text{TiCl}_4}^0$ is the partial pressure when TiCl_4 is in the gas phase. E_0 is the average activation energy at the temperature of 250~550 °C.

A typical first-order reaction rate kinetic equation can be obtained, indicating that CVD process of TiO_2 is a kinetic-controlled process. The establishment of the kinetic equation provides guidance for the process design of CVD in loading TiO_2 .

3 Conclusions

1) The surface of modified cordierite with TiO_2 is mainly composed of (211)-oriented and (200)-oriented anatase- TiO_2 which is in octahedron and cube forms with the Brunauer-Emmett-Teller (BET) specific surface area of $78.80 \text{ m}^2 \cdot \text{g}^{-1}$, an average pore diameter of 9.80 nm, and a bimodal distribution. These components can provide good structure condition for subsequent loading of active components.

2) The chemical vapor deposition (CVD) process of TiO_2 is mainly the diffusion and mass transfer adsorption of TiCl_4 and O_2 to the cordierite matrix. TiCl_4 decomposes and enters the cordierite matrix under high oxygen potential to form TiO_2 nuclei which suffer the preferential orientation and epitaxial growth.

3) The loading reaction of TiO_2 on cordierite is related to the temperature and the partial pressure of the components in the system, and is controlled by kinetics. The activation energy of the reaction is 60.3 kJ/mol, and the deposition rate equation is $V = 6807 \exp\left(-\frac{7255}{T}\right) P_{\text{TiCl}_4}^0$. The kinetic model can provide guidance for further mechanism investigation and CVD process design.

References

- Weng X L, Xue Y H, Chen J K. *Journal of Hazardous Materials* [J], 2020, 387: 121 705
- Xu Y F, Wu X D, Lin Q W et al. *Applied Catalysis A: General* [J], 2019, 570: 42
- Wu Shiguo, Zhang Lei, Wang Xiaobo et al. *Applied Catalysis A: General*[J], 2015, 505: 235
- Qi Chunping, Bao Weijun, Wang Liguang et al. *Catalysts*[J], 2017, 7(12): 110
- Meunier F C, Zuzaniuk V, Breen J P et al. *Catalysis Today*[J], 2000, 59(3-4): 287
- Paukshits E A. *Journal of Molecular Catalysis A: Chemical*[J], 2000, 158(1): 37
- Richard G, Herman, John W. *Topics in Catalysis*[J], 2002, 18(3-4): 251
- Shen S C, Kawi S. *Catalysis Today*[J], 2001, 68(1-3): 245
- Li Q C, Chen S F, Liu Z Y et al. *Applied Catalysis B: Environmental*[J], 2015, 164: 475
- Li Xiang, Li Xiansheng, Chen Jianjun et al. *Catalysis Communications*[J], 2016, 87: 45
- Kong M, Liu Q, Jiang L et al. *Chemical Engineering Journal*[J], 2019, 370: 518
- Cao Jun, Yao Xiaojiang, Chen Li et al. *Journal of Rare Earths* [J], 2020, 38(11): 1207
- Chen Hongfeng, Xia Yang, Fang Ruyi et al. *Applied Surface Science*[J], 2018, 459: 639
- Xiao Haiping, Dou Chaozong, Shi Hao et al. *Catalysts*[J], 2018, 8(11): 541
- Hu Guang, Yang Jian, Tian Yuanmeng et al. *Materials Research Bulletin*[J], 2018, 104: 112
- Wang Hongyan, Wang Baodong, Sun Qi et al. *Catalysis Communications*[J], 2017, 100: 169
- Chen Mengyin, Zhao Mengmeng, Tang Fushun et al. *Journal of Rare Earths*[J], 2017, 35(12): 1206
- Ma Ziran, Wu Xiaodong, Feng Ya et al. *Progress in Natural Science: Materials International*[J], 2015, 25(4): 342
- Chen J, Mei L F, Liao L B. *Key Engineering Materials*[J], 2012, 512-515: 1686
- Huang D, Liu Q, Miyamoto Y et al. *Journal of Porous Materials* [J], 2012, 19(6): 1003
- Yang Mei, Tang Ning, Huang Yuting et al. *Rare Metal Materials and Engineering*[J]. 2020, 49(2): 404
- See C H, Harris A T. *Industrial & Engineering Chemistry Research*[J], 2007, 46(4): 997
- Woods J, Beach D, Nygren C et al. *Chemical Vapor Deposition* [J], 2005, 11(6-7): 289
- Wang H S, Yun T S, Zhu G S et al. *Rare Metal Materials and Engineering*[J], 2016, 45(12): 3121
- Kuo D H, Shueh C N. *Chemical Vapor Deposition*[J], 2003, 9(5): 265

堇青石表面化学气相沉积二氧化钛的负载机理及负载动力学

杨 眉¹, 刘良文¹, 郑 珩², 卢静祥¹, 王静怡¹

(1. 西南石油大学 新能源与材料学院, 四川 成都 610500)

(2. 西南化工研究设计院 工业废气再利用国家重点实验室, 四川 成都 610225)

摘要: 以酸蚀改性堇青石为基体, 利用化学气相沉积法 (CVD) 在基体上负载 TiO_2 , 采用扫描电子显微镜、能谱仪、X射线衍射仪、BET 比表面积法等对负载了 TiO_2 的堇青石进行表征, 测定不同温度下的负载速度。结果表明: 负载了 TiO_2 的堇青石主要由 (211) 及 (200) 取向的锐钛矿 TiO_2 组成, 呈八面体和立方体形态, BET 比表面积达 $78.80 \text{ m}^2 \cdot \text{g}^{-1}$, 平均孔径为 9.80 nm, 具有双峰分布特征。负载过程为 TiCl_4 及 O_2 向堇青石基体扩散吸附, TiCl_4 分解为 Ti^{4+} 并在高氧势下进入基体晶格形成 TiO_2 晶核, 并经过择优取向和外延式生长, 其负载沉积速率方程为 $V = 6807 \exp\left(-\frac{7255}{T}\right) P_{\text{TiCl}_4}^0$, 其中 T 为负载温度, $P_{\text{TiCl}_4}^0$ 为气相 TiCl_4 的分压。

关键词: 催化剂; SCR; CVD; TiO_2 ; 负载动力学

作者简介: 杨 眉, 男, 1971 年生, 博士, 教授, 西南石油大学新能源与材料学院, 四川 成都 610500, E-mail: 199631010016@swpu.edu.cn